



Epstein–Barr virus-encoded miR-BART5-5p upregulates PD-L1 through PIAS3/pSTAT3 modulation, worsening clinical outcomes of PD-L1-positive gastric carcinomas

Chan Jin Yoon¹ · Mee Soo Chang² · Dong Ha Kim¹ · Won Kim³ · Bo Kyung Koo³ · Sung-Cheol Yun⁴ · Sung Han Kim¹ · Yang Soo Kim¹ · Jun Hee Woo¹

Received: 4 November 2019 / Accepted: 8 March 2020 / Published online: 23 March 2020
© The International Gastric Cancer Association and The Japanese Gastric Cancer Association 2020

Abstract

Background Epstein–Barr virus (EBV) is etiologically associated with ~ 10% of all gastric carcinomas. However, the molecular mechanisms and roles of EBV miRNAs in gastric carcinoma oncogenesis are yet to be elucidated.

Methods MicroRNA microarray and TaqMan quantitative real-time RT-PCR were conducted. RT-PCR and luciferase reporter assay for PIAS3, western blotting for 20 proteins, immunofluorescence for STAT3, transfection with miRBART5-5p-plasmid, STAT3-plasmid, miRBART5-5p mimic, or PIAS3-siRNA, and in vitro assays for biological effects of PD-L1 were implemented. In situ hybridization for EBV-encoded small RNAs and immunohistochemistry were performed on gastric carcinoma tissues.

Results Transfecting miR-BART5-5p into EBV(–) gastric carcinoma cell lines caused a decrease in PIAS3 3'-UTR reporter activity, PIAS3 downregulation, and subsequent STAT3 activation followed by PIAS3/pSTAT3-dependent PD-L1 upregulation. Interestingly, due to PD-L1 knockdown, apoptosis was increased, while the rate of cell proliferation, invasion capacity, and migration were decreased in miR-BART5-5p-transfected cells. In EBV(+) gastric carcinoma cells, anti-miR-BART5-5p reduced PD-L1 levels through PIAS3/pSTAT3 control. Among 103 patients with EBV-associated gastric carcinomas, overall survival was significantly shortened for those with PD-L1(+) tumors compared to those with PD-L1(–) tumors ($P=0.049$).

Conclusions Our findings imply that miR-BART5-5p directly targets PIAS3 and augments PD-L1 through miR-BART5/PIAS3/pSTAT3/PD-L1 axis control. This contributes to antiapoptosis, tumor cell proliferation, invasion and migration, as well as immune escape, furthering gastric carcinoma progression and worsening the clinical outcome, especially in the PD-L1(+) group of patients with EBV-associated gastric carcinomas. miR-BART5-5p may, therefore, be amenable to PD-1/PD-L1 immune checkpoint inhibitor therapy.

Keywords Epstein–Barr virus · miR-BART5 · PIAS3 · pSTAT3 · PD-L1 · Gastric carcinoma

Chan Jin Yoon and Mee Soo Chang contributed equally to this work.

Electronic supplementary material The online version of this article (<https://doi.org/10.1007/s10120-020-01059-3>) contains supplementary material, which is available to authorized users.

✉ Mee Soo Chang
meesooch@snu.ac.kr

✉ Jun Hee Woo
junheewoo@amc.seoul.kr

Extended author information available on the last page of the article

Introduction

The Epstein–Barr virus (EBV) is a ubiquitous human herpes virus that infects more than 90% of the world's adult population [1]. In certain circumstances, EBV can also act as an oncogenic virus. For instance, it can cause Burkitt lymphoma, Hodgkin's disease, nasal NK/T cell lymphoma, nasopharyngeal carcinoma, and gastric carcinoma [2]. In Korea, gastric carcinoma is the most prevalent malignancy, and the third highest cause of cancer-related death [3]. EBV infection has been detected in approximately 5–10% of all gastric carcinoma cases worldwide, irrespective of whether it is endemic to particular countries or geographical regions [4]. Accumulating evidence corroborates that EBV-associated gastric carcinoma

is a distinct subset of gastric carcinomas, both clinicopathologically and molecularly. They are characterized by extreme CpG hypermethylation throughout the genome [5], frequent mutations in *PIK3CA* [5] and *ARID1A* [6], lack of *TP53* mutations [5], and overexpression of interferon- γ [7] and PD-L1 [5, 8].

MicroRNAs (miRNAs) are a family of endogenous, non-coding RNAs that are 17–23 nucleotides long and bind to complementary sites in the 3'-untranslated regions (3'-UTRs) of target mRNAs, blocking or repressing protein translation [9]. First described in 2004 [10], EBV-encoded miRNAs are located in two regions of the EBV genome: BamHI-A rightward transcripts (BART) (encoding 40 mature miRNAs) and BHRF1 (encoding four mature miRNAs) [1, 9]. EBV positive (EBV(+)) gastric carcinoma cells express BART miRNAs, but no BHRF1 miRNAs [11, 12]. Emerging evidence shows that EBV miRNAs target multiple human mRNAs, and downregulate proteins relevant to cell proliferation, apoptosis, human immune function, and cytokine signaling [13]. In gastric carcinoma cells, miR-BART5 inhibits apoptosis by targeting PUMA [14] and TP53 [15], and miR-BART20-5p promotes cell proliferation and suppresses apoptosis by targeting BAD [16]. Unexpectedly, however, miR-BART15-3p enhances apoptosis by targeting BRUCE [17]. In nasopharyngeal carcinoma cells, miR-BART1 promotes metastasis via the PTEN pathway [18], miR-BART3 enhances growth and transformation by targeting the tumor suppressor DICE1 [19], miR-BART6-3p targets RIG-I and suppresses IFN- β production [20], miR-BART8-3p targets RNF38 and promotes metastasis [21], miR-BART9 promotes metastasis by targeting E-cadherin [22], and miR-BART10-3p enhances metastasis by targeting BTRC [23]. However, the targets and roles of most EBV BART miRNAs remain largely uncharacterized in the context of gastric carcinoma.

In this study, we investigated the cellular target of miR-BART5-5p and its role as a viral onco-miRNA. We found that EBV miR-BART5-5p directly targets PIAS3 and upregulates programmed death-ligand 1 (PD-L1) through miR-BART5/PIAS3/pSTAT3/PD-L1 axis control. As PD-L1 is involved in antiapoptosis and immune escape, its expression may contribute to unfavorable clinical outcomes in patients with EBV-associated gastric carcinoma. Our findings shed new light on the intrinsic mechanisms of PD-L1 upregulation by a viral miRNA in EBV(+) gastric carcinomas and rationalize PD-1/PD-L1 immune checkpoint inhibitors as potential therapeutics for the treatment of EBV-associated gastric carcinoma.

Materials and methods

Cell culture

In our study, we used five gastric carcinoma cell lines established from gastric tumors of five individual patients.

SNU601, SNU484, SNU216, and SNU719 were acquired from the Korean Cell Line Bank (Seoul, Korea). YCCEL1 was provided by Dr. SY Rha [24]. SNU601, SNU484, and SNU216 are EBV(-); SNU719 and YCCEL1 are EBV(+). HEK293T cell line was purchased from the American Type Culture Collection (Manassas, VA, USA). Cells were cultured in RPMI 1640 medium (Gibco BRL, Rockville, MD, USA) supplemented with 10% fetal bovine serum and antibiotics (100 U/mL penicillin and streptomycin) at 37 °C in an atmosphere of 5% CO₂.

MicroRNA microarray analysis

The miRNA expression profiles of gastric carcinoma were conducted with the SurePrint G3 Human miRNA Microarray, Release 16.0, 8 × 60 K (Agilent Technologies, Santa Clara, CA, USA) that contains a total of 1205 human and 144 viral miRNAs. Array data export processing and analysis was performed using Affymetrix GeneChip Command Console Software. Quantile normalization was conducted using statistical computing program, R version 3.0.2 (<https://www.r-project.org>) to standardize the data across the samples [25]. For ebv-miRNAs, relative expression levels were determined by “each EBV miRNA level/ebv-miR-BART5-3p level”. Additionally, hsa-miRNAs data of EBV(+) gastric carcinomas and EBV(-) gastric carcinomas were compared using threshold values of ≥ 1.5 -fold change, and corrected *P* value < 0.05. Hierarchical clustering was then achieved using the Euclidean distance metric and the complete linkage rule.

Total RNA (including miRNAs) was extracted from formalin-fixed, paraffin-embedded tissue blocks using the miRNeasy FFPE kit (Qiagen, Hilden, Germany). Tissue lysates were treated with DNase I (Roche, Basel, Switzerland) to eliminate DNA contamination.

Reverse transcription-polymerase chain reaction (RT-PCR)

Total RNA was extracted using an RNeasy Mini Kit (Qiagen). Extracted RNA was treated for 20 min at 37 °C with 10 units of DNase I (Roche) and an RNase inhibitor (Roche) to eliminate remaining genomic DNA. After inactivation at 75 °C for 10 min, RNA samples were purified with an RNeasy Mini Kit (Qiagen). Complementary DNA (cDNA) was synthesized from 1 μ g of total RNA with a high-fidelity RT-PCR system. The following primers were used for cDNA amplification: PIAS3 (forward, 5'-GCACCCTGATGTCACCATGA-3'; reverse, 5'-CATTGGCTCCTGGCAGAAC-3'), β -actin (forward, 5'-GACAGGATGCAGAAGGAGATTACT-3'; reverse, 5'-TGATCCACATCTGCTGGAAGGT-3').

Quantitative real-time RT-PCR

Total RNA (including miRNAs) was extracted using the miRNeasy Mini Kit (Qiagen). miRNA cDNA was synthesized with 10 ng of total RNA from each sample using the TaqMan MicroRNA Reverse Transcription Kit (Ambion Life Technologies, Grand Island, NY, USA). TaqMan quantitative real-time RT-PCR analysis was conducted with an ABI 7900 Real-Time PCR System using the TaqMan miRNA assay with the EBV-miR-BART5-5p (MIMAT0003413), EBV-miR-BART10-3p (MIMAT0003420), EBV-miR-BART22 (MIMAT0010132) or hsa-miR-18a (MIMAT0000072) primer sets (Applied Biosystems, Foster City, CA, USA), according to the manufacturer's protocol. RNU6b (Applied Biosystems) was utilized to normalize microRNA expression.

Western blotting and densitometric analysis

Proteins were separated by SDS-PAGE using a 5% stacking gel, and then transferred onto reinforced PVDF membranes (Millipore, Bedford, MA, USA). After blocking the non-specific sites, each membrane was probed overnight at 4 °C with one of the following primary antibodies: PIAS3 (D5F9, 1:1000), STAT3 (124H6, 1:1000), phospho-STAT3 (D3A7, 1:1000), phospho-Akt (D9E, 1:1000), Akt (11E7, 1:1000), phospho-mTOR (Ser2448, 1:1000), poly ADP ribose polymerase (PARP) (#9542, 1:1000), Cyclin D1 (92G2, 1:1000), Cyclin D3 (DCS22, 1:1000), CDK2 (78B2, 1:1000), CDK4 (D9G3E, 1:1000), and CDK6 (DCS83, 1:1000) from Cell Signaling (Beverly, MA, USA); PD-L1 (17952-1-AP, 1:1000) from Proteintech Fisher Scientific (Hampton, NH, USA); NF- κ B p65 (A, 1:500), mTOR (30, 1:1000), c-Myc (9E11, 1:1000), c-Jun (H-79, 1:1000), caspase-3 (H-277, 1:1000), MMP2 (H-76, 1:1000), MMP9 (2C3, 1:1000), and transcription factor IIB (sc-23875, 1:2000) from Santa Cruz Biotechnology (Santa Cruz, CA, USA); and MMP1 (ab53142, 1:1000) and β -actin (AC-15, 1:10,000) from Abcam (Cambridge, UK). The membranes were washed and incubated for 30 min at room temperature with horseradish peroxidase-conjugated anti-mouse or anti-rabbit secondary antibodies (Cell Signaling). An antibody against β -actin (AC-15, 1:10,000, Abcam) or transcription factor II B (sc-23875, 1:2000, Santa Cruz Biotechnology) was used to confirm equal loading and transfer of each protein from total cellular extracts or nuclear extracts.

Western blots were digitalized using the GS-700 Imaging Densitometer (Bio-Rad, Hercules, CA, USA), processed with Corel Photo Paint 7.0 to adjust image brightness and contrast. The densities of western blots were evaluated using Molecular Analyst Software (Bio-Rad), and normalized to pertinent controls.

For extraction of nuclear protein only, we utilized lysis buffer A (10 mol/L Tris, pH 8.0, 60 mmol/L NaCl, 1 mmol/L EDTA, 1 mmol/L dithiothreitol, 0.1% Nonidet P-40, and 1 mmol/L phenylmethylsulfonyl fluoride) and buffer B (200 mmol/L HEPES, pH 7.9, 0.75 mmol/L spermidine, 0.15 mmol/L spermine, 0.2 mmol/L EDTA, 2 mmol/L EGTA, 2 mmol/L dithiothreitol, 20% glycerol, 1 mmol/L phenylmethylsulfonyl fluoride, and 0.4 M NaCl), as previously described [26].

MicroRNA, plasmid and small interfering RNA transfection, and inhibitor treatment

The pTRIPZ-miR-BART5 plasmid was a kind gift from Professor Bryan R. Cullen (Duke University). EBV-miR-BART5-5p mimic (miR-BART5-5p; MC11615), EBV-miR-BART5-5p inhibitor (Anti-miR-BART5-5p; MH11615), EBV-miR-BART10-3p mimic (miR-BART10-3p; MC12577), EBV-miR-BART10-3p inhibitor (Anti-miR-BART10-3p; MH12577), EBV-miR-BART22 mimic (miR-BART22; MC15462), EBV-miR-BART22 inhibitor (Anti-miR-BART22; MH15462), and the scrambled miRNA control (miR-control) were from Ambion Applied Biosystems (Austin, TX, USA), and hsa-miR-18a-5p mimic (Pre-miRTM miRNA Precursor; AM17100), hsa-miR-18a-5p inhibitor (Anti-miRTM miRNA Inhibitor; AM17000), from the Bioneer (Daejeon, Republic of Korea). They were transfected at a final concentration of 1 nM using Lipofectamine 2000 (Invitrogen, Carlsbad, CA, USA).

The pPM-C-His-PIAS3 plasmid and the pcDNA3-STAT3 plasmid were obtained from Applied Biological Materials Inc. (Richmond, BC, Canada) and Addgene (Cambridge, MA, USA), respectively. Cells were transfected with 4 μ g plasmid DNA using Lipofectamine 2000 (Invitrogen) in 500 μ L serum-free medium for 4 h at 37 °C in a CO₂ incubator per manufacturer's instructions.

PIAS3-specific small interfering RNA (siRNA) (AM16704; 5'-GGAUGUAAGGCCUUAGCCA-3') and PD-L1-specific siRNA (s26547; 5'-GGCAUUUGCUGA ACGCAUU-3') were synthesized by Ambion Applied Biosystems. A scrambled siRNA (sc-37007, Santa Cruz Biotechnology) was used as the negative control. Cells were transfected with 200 pmol siRNA using Lipofectamine 2000 (Invitrogen) in 3 mL serum-free medium for 4 h at 37 °C in a CO₂ incubator per manufacturer's instructions. Without removing the transfection mixture, 3 mL RPMI with 20% fetal bovine serum was added. Cells were incubated for an additional 24 h.

For STAT3 knockdown, cells were incubated with the STAT3 inhibitor, S3I-201 (Sigma-Aldrich, St. Louis, MO, USA), at 100 μ M for 24 h.

Luciferase activity assay for PIAS3

The entire 3-UTR of PIAS3 was cloned into the pEZX-MT06 vector to generate a luciferase reporter gene containing the seed match for miR-BART5-5p. HEK293T cells were co-transfected with 0.8 µg of pEZX-MT06 vector including either the PIAS3 3-UTR *Renilla*/firefly dual-luciferase reporter plasmid or the empty vector (GeneCopoeia, Rockville, MD, USA); and with the miR-BART5-5p mimic or scrambled miRNA control (miR-control). After 48 h, luciferase activity was calculated using the dual-luciferase assay kit (Promega, Madison, WI, USA). *Renilla* luciferase activity was normalized to firefly luciferase activity. All assays were performed in triplicate, and each transfection with the reporter plasmid was conducted on a separate day.

Immunofluorescence assay

Cells grown on coverslips were fixed for 10 min in 4% paraformaldehyde in 10 mmol/L piperazine- N,N-bis (2-ethanesulfonic acid) (PIPES), pH 6.8, 10 mmol/L NaCl, 300 mmol/L sucrose, 3 mmol/L MgCl₂, and 2 mmol/L EDTA. Cells were immersed for 10 min in Tris-buffered saline (TBS) with 0.75% Triton X-100, and blocked for 10 min with 5% bovine serum albumin and 0.1% Triton X-100 in TBS. Cells were then incubated with a primary antibody against STAT3 (124H6, 1:200, Cell Signaling, Beverly, MA, USA) and an Alexa Fluor 488-conjugated goat anti-mouse IgG (H+L) secondary antibody (Invitrogen, Carlsbad, CA, USA). Nuclei were counterstained with 4,6-diamidino-2-phenylindole (DAPI) (1 µg/mL). Stained cells were visualized on a Zeiss Observer Z1 fluorescence microscope (Carl Zeiss Meditec AG, Jena, Germany).

Apoptosis, cell proliferation, invasion, and migration assays

Apoptosis was evaluated with the annexin V-fluorescein isothiocyanate (FITC) apoptosis kit (BD Biosciences, San Diego, CA, USA) as stated in the manufacturer's protocol. Briefly, cells were cultured in serum-free medium, trypsinized, centrifuged, and resuspended in annexin V-binding buffer (150 mmol/L NaCl, 18 mmol/L CaCl₂, 10 nmol/L HEPES, 5 mmol/L KCl, and 1 mmol/L MgCl₂). The cells were stained with FITC-conjugated annexin V (1 µg/mL) and propidium iodide (50 µg/mL), and promptly analyzed on a FACScan flow cytometer (Becton Dickinson, Mountain View, CA, USA) installed with the CellQuest software (Becton Dickinson).

Cell proliferation was measured with the Cell Counting Kit-8 (CCK-8; Dojindo Laboratories, Kumamoto, Japan).

Absorbance was measured at A₄₅₀ nm on a spectrophotometer (Spectramax 190; Molecular Devices, Sunnyvale, CA, USA).

Cell invasion was evaluated with 6-well BioCoat Matrigel invasion chambers (BD Biosciences) according to the manufacturer's protocol, with minor modifications. Briefly, cells (1 × 10⁵) in 200 µL medium were plated in the upper chamber, and the lower chamber was filled with 1 mL serum-free medium supplemented with 10% bovine serum albumin. After incubation for 24 h at 37 °C, cells that invaded the lower chamber were stained with 8 µg/mL calcein AM (BD Biosciences) in Hanks' buffered saline at 37 °C for 30 min and counted on a fluorescence microscope (Olympus IX71; Tokyo, Japan).

Cell migration was examined with a wound-healing assay. Briefly, using the tip of a micropipette, a plate of confluent cells was scratched to create the "wound" (an area free of cells). Images were captured at 0 h, 24 h, and 48 h with an inverted photomicroscope (Olympus IX71), and movements of individual cells were calculated with NIH Image J software (<https://rsb.info.nih.gov/ij/index.html>).

RNA in situ hybridization and immunohistochemistry of surgically resected gastric carcinoma tissues

We included 103 specimens of EBV-associated gastric carcinoma tissue acquired during surgical resection from 1997 to January 2013 at the Seoul National University Boramae Hospital. Overall survival of patients was estimated from the date of surgery to death or to the last follow-up visit. Median follow-up period for overall survival was 59 months (mean ± SD: 60.5 ± 36.14, range: 1–130).

In situ hybridization for EBV-encoded small RNAs (EBERs) and immunohistochemistry were performed on formalin-fixed, paraffin-embedded tissues using an automated immunostainer, the BenchMark Ultra IHC/ISH system (Ventana Medical Systems, Tucson, AZ, USA) per the manufacturer's instructions. The INFORM EBER probe (Ventana Medical Systems) was used for EBER in situ hybridization. EBV-infected cells were detected as black signals at the hybridization site using light microscopy. All EBV-positive cases revealed black signals in almost all cancer cell nuclei.

To assess PIAS3, pSTAT3, and PD-L1 expression by immunohistochemistry, tissues were incubated with anti-PIAS3 (ab119106, 1:50, Abcam), phospho-STAT3 (Tyr705) (1:50, Cell Signaling), or PD-L1 antibody (SP263, ready to use, Ventana Medical Systems). For statistical evaluation in interpretation of immunohistochemical staining results, a two-tiered system was adopted; positive vs. negative (for pSTAT3 and PD-L1), or retention vs. loss (for PIAS3). Hence, PIAS3 should be retained as a normal feature [27]. If ≥ 5% of tumor cells in a tissue

section displayed reactivity, the tissue was considered positive for pSTAT3 or PD-L1 and retained for PIAS3.

Statistical analysis

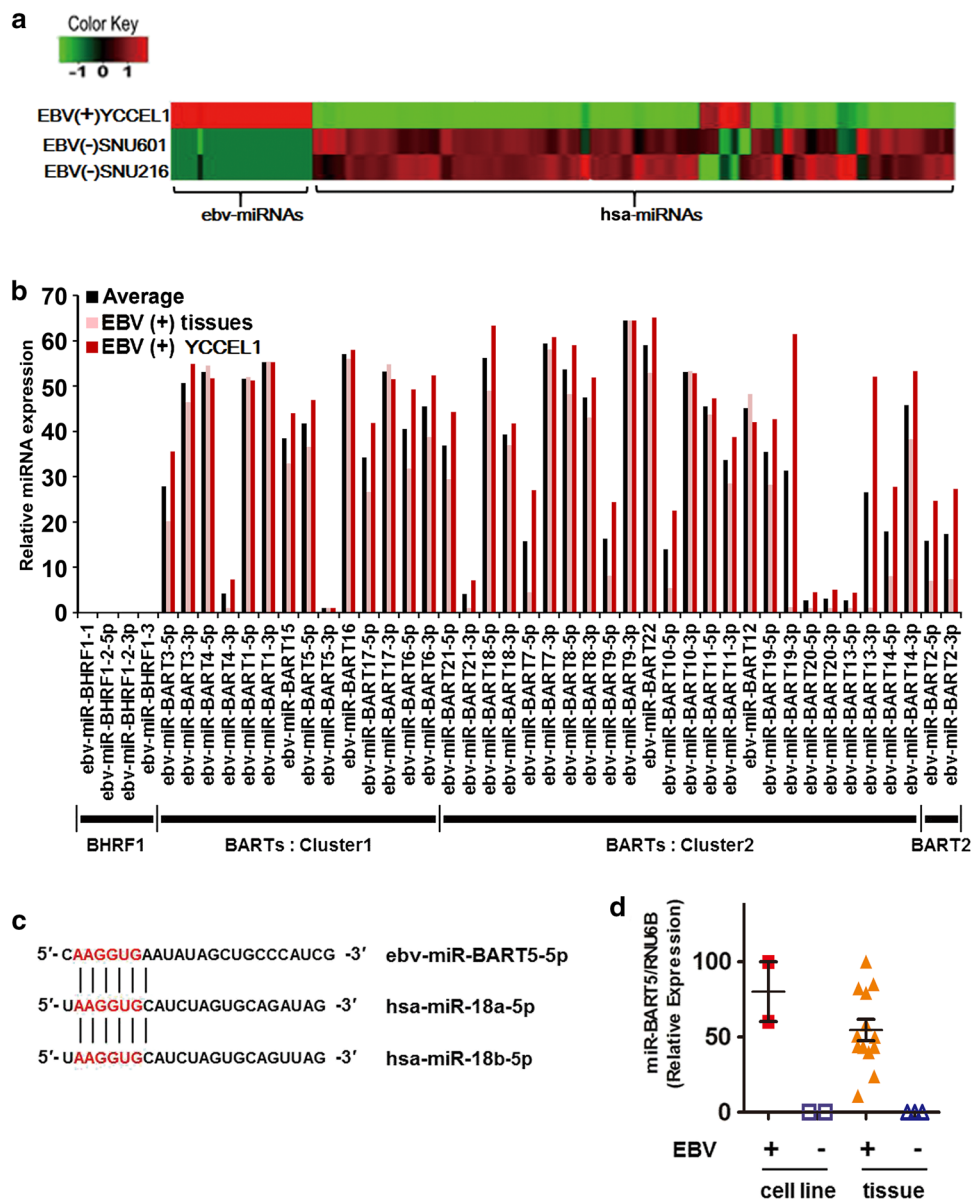
Chi-square test, Pearson's test, two-tailed Student's *t* test, Spearman's rank correlation coefficient analysis, and Kaplan–Meier survival analysis were conducted with IBM® SPSS® Statistics 20.0 (IBM Inc., Chicago, IL, USA). *P* < 0.05 was considered statistically significant.

Results

miR-BART5-5p is expressed in EBV(+) gastric carcinoma cells and EBV(+) gastric carcinoma tumor samples

We found that miRNAs were differentially expressed according to EBV status. By comparing differential expression with a 1.5-fold difference between EBV(+) and EBV(−) cells, 132 cellular miRNAs were found to be downregulated, while 59 cellular miRNAs were upregulated in EBV(+) cells vs. EBV(−) cells. EBV-encoded miRNAs were only expressed in the EBV(+) gastric carcinoma cell line (Fig. 1a). Forty EBV-encoded miRNAs

Fig. 1 MicroRNA (miRNA) microarray expression profile and miR-BART5-5p expression in gastric carcinoma cell lines and gastric carcinoma tissue samples. **a** Heat map and hierarchical clustering of Epstein–Barr virus (EBV) miRNAs (ebv-miRNAs) and human miRNAs (hsa-miRNAs) expressed by gastric carcinoma cell lines that are “EBV(+) YCCEL1” or “EBV(−) SNU601” and “EBV(−) SNU216”. **b** Relative expression levels of each ebv-miRNA (each EBV miRNA level/ebv-miR-BART5-3p level) in EBV(+) gastric carcinoma tissues (*n* = 3; the average miRNA profiles in three samples) (pink bars), EBV(+) gastric carcinoma cell line (*n* = 1) (red bars), and the average miRNA profiles in tissues and cells (black bars). **c** Seed sequence homology of miR-BART5-5p with hsa-miR-18a and hsa-miR-18b. **d** Relative expression of miR-BART5-5p by qRT-PCR in the EBV(+) gastric carcinoma YCCEL1 cell line and SNU719 cell line (*n* = 2) vs. EBV(−) SNU601 and SNU216 cell lines (*n* = 2), and in EBV(+) gastric carcinoma tissue (*n* = 13) vs. EBV(−) gastric carcinoma tissue samples (*n* = 3). Expression levels were normalized to RNU6B. Data represent mean ± SD



were expressed in the EBV(+) gastric carcinoma cell line and EBV(+) gastric carcinoma tumor tissues samples, and all 40 mapped to either the miR-BART cluster 1 or miR-BART cluster 2. BHRF miRNAs were not expressed by any of the cell lines or tissue samples examined (Fig. 1b).

To identify the human cellular targets of EBV-miRNAs, we referred to the literature, and carried out computational screening using data in the miRbase database (<https://www.mirbase.org>) and the VIRmiRNA database (<https://crdd.osdd.net/servers/virmirna/seed-align.html>). We recognized that 13 EBV-miRNAs had seed sequence homology with 21 human onco-miRNAs [28]. Among these EBV-miRNAs, we focused on miR-BART5-5p to determine whether miR-BART5-5p has cancer-associated function, despite its considerably low level in our microRNA microarray data of gastric carcinomas, which is different from the findings of Choy et al., who showed an abundance of miR-BART5-5p [14]. We found that miR-BART5-5p had seed sequence homology with two human miRNAs, hsa-miR-18a-5p, and hsa-miR-18b-5p (Fig. 1c), which are associated with cancer [29]. We verified the expression of miR-BART5-5p in EBV(+) gastric carcinoma cells and tissues compared to EBV(-) cell lines and tissues using qRT-PCR (Fig. 1d).

Construction of miR-BART5-5p stably-expressing cells and optimization of miR-BART5-5p-mimic transfection

To explore the specific role of miR-BART5-5p in the development of gastric carcinoma, we sought to establish gastric carcinoma cell lines that stably express miR-BART5-5p, and no other EBV-encoded miRNAs. To this end, we transfected the pTRIPZ-miR-BART5-5p plasmid (a kind gift from Professor Bryan R. Cullen, Duke University) into EBV(-) gastric carcinoma SNU601 and SNU216 cell lines. Among the cell lines established, miR-BART5-5p was expressed at levels significantly lower (at best, 222-fold lower) than that of SNU719 and YCCEL1 cells, which reflect the typical expression levels of cell lines derived from naturally occurring EBV(+) gastric carcinoma tumors (S1 Fig.). To achieve levels that more closely mimic endogenous expression, we chose to use a commercially available EBV-miR-BART5-5p mimic. First, we transfected various concentrations (1, 10, 25, and 50 nM) of the mimic into EBV(-) gastric carcinoma SNU601 cells. After 48 h, we assessed its expression by qRT-PCR. Finally, we determined that 1 nM was the optimal transfection concentration of the miR-BART5-5p mimic, because miR-BART5-5p expression levels in 1 nM-transfected cells most closely reflected endogenous expression (S2A Fig.), and transfection stress, cell damage, etc., were minimal (S2B Fig.).

miR-BART5-5p directly targets PIAS3 and reduces PIAS3 protein levels

Since hsa-miR-18a-5p directly targets the protein inhibitor of activated signal transducer and activator of transcription 3 (PIAS3) [30], and miR-BART5-5p shows seed homology with has-miR-18a-5p, we investigated whether miR-BART5-5p may also target PIAS3. In the original naive cell lines, PIAS3 protein levels were lower in EBV(+) gastric carcinoma cell lines (SNU719 and YCCEL1, endogenously expressing miR-BART5-5p) than in EBV(-) cell lines (SNU216, SNU484, and SNU601, not expressing miR-BART5-5p) (Fig. 2a, b). Specifically, there was an inverse correlation between levels of miR-BART5-5p and PIAS3 protein in gastric carcinoma cell lines ($P = 0.068$) (Fig. 2c).

To confirm miR-BART5-5p-induced PIAS3 down-regulation, we transfected miR-BART5-5p into SNU216, SNU484, and SNU601 cells (EBV(-) gastric carcinoma cell lines), and anti-miR-BART5 into YCCEL1 (an EBV(+) gastric carcinoma cell line) (Fig. 2d). PIAS3 mRNA levels were unaltered in all examined cell lines, irrespective of miR-BART5-5p (Fig. 2e). PIAS3 protein levels were lower in miR-BART5-5p-transfected gastric carcinoma cells than in their corresponding miR-control-transfected cells. Conversely, PIAS3 protein levels were higher in anti-miR-BART5-transfected YCCEL1 cells than in the corresponding miR-control-transfected cells ($P < 0.05$, each) (Fig. 2f).

Furthermore, comparing RNA sequences, the 3-UTR of PIAS3 was found to contain a potential binding site for miR-BART5-5p, and relative luciferase activity diminished significantly in HEK293T cells co-transfected with a plasmid containing the 3-UTR of PIAS3 and miR-BART5-5p, compared to that in HEK293T cells co-transfected with a negative control (empty vector) and miR-BART5-5p (Fig. 2g). These results indicate that PIAS3 reduction was directly driven by miR-BART5-5p.

To evaluate the effect of miR-BART5-5p on the expression of proteins besides PIAS3, we tested 18 proteins related to gastric oncogenesis such as NF- κ B, apoptosis indicators, Akt/mammalian target of rapamycin (mTOR) signaling, matrix metalloproteinase (MMP) family, and cell cycle-related proteins. We transfected miR-BART5-5p into EBV(-) gastric carcinoma SNU216 cells and SNU601 cells, or with anti-miR-BART5-5p into EBV(+) gastric carcinoma YCCEL1 cells and SNU719 cells. After 48 h, proteins from nuclear extracts and/or total cellular extracts were harvested for western blotting. We found that levels of these proteins were not modified by miR-BART5-5p or anti-miR-BART5-5p (S3 Fig.).

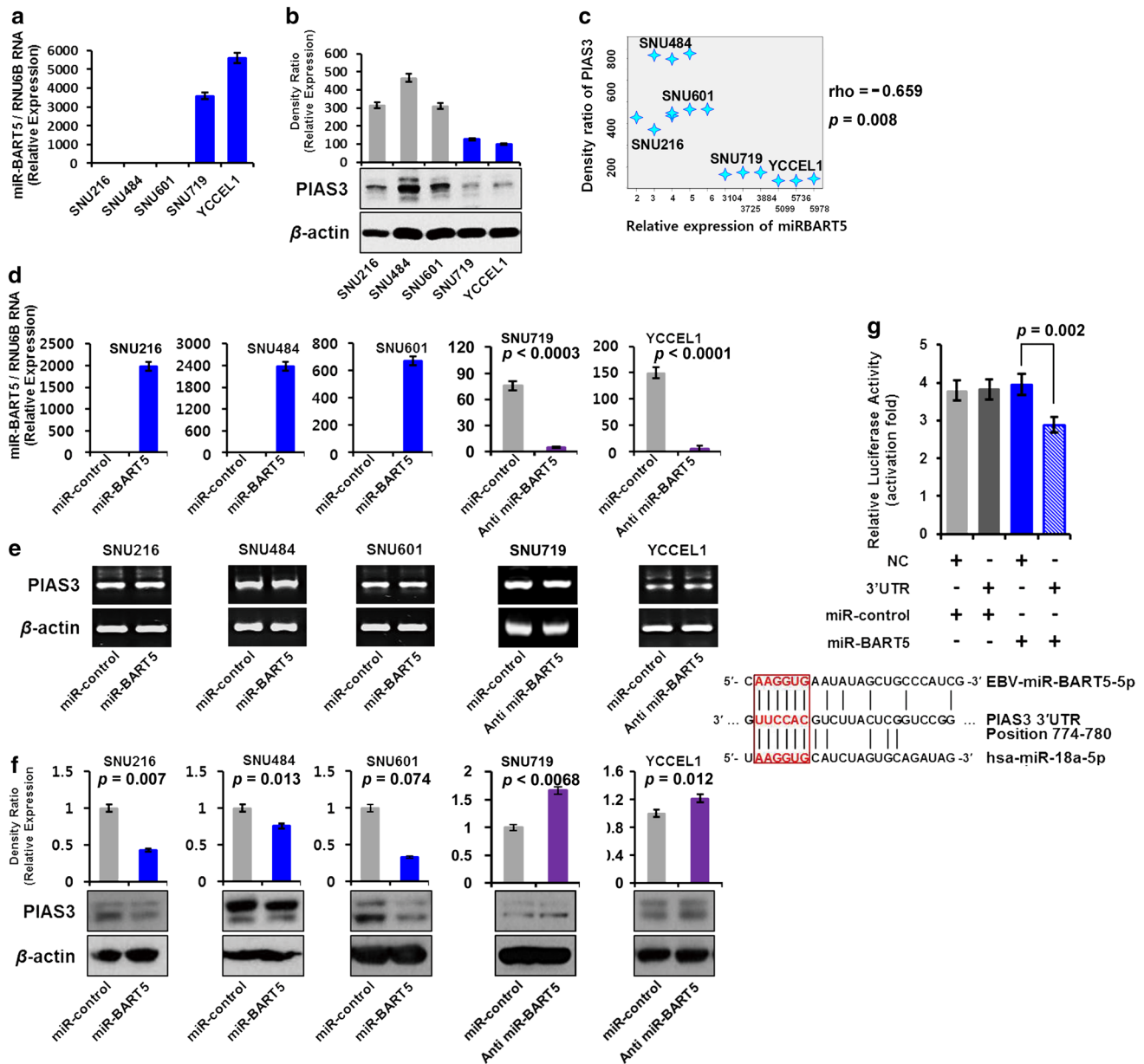


Fig. 2 miR-BART5-5p downregulates the expression of PIAS3 by directly targeting PIAS3. **a–c** Inverse correlation between miR-BART5-5 level and PIAS3 protein level in original naive cells (without any transfection or treatment). **a** Relative expression of miR-BART5-5p in EBV(+) gastric carcinoma cell lines (SNU719 and YCCEL1), and EBV(–) gastric carcinoma cell lines (SNU216, SNU484, and SNU601) by qRT-PCR. Expression levels were normalized to RNU6B RNA. **b** Expression of PIAS3 in the aforementioned (original naive) cell lines by western blot analysis. Representative images (bottom) and quantification of PIAS3 expression by densitometry (bar graph). The bar graph shows PIAS3 normalized to β -actin. EBV(–) gastric carcinoma cell lines are represented as black columns, and EBV(+) gastric carcinoma cell lines as gray columns. **c** Inverse correlation between miR-BART5-5 level (**a**) and PIAS3 protein level (**b**) was deduced by Spearman's rho ($\rho = -0.659$, $P = 0.008$) in five cell lines. **d–f** miR-BART5-5p-induced PIAS3 downregulation. **d** miR-BART5-5p levels in EBV(–) SNU216,

SNU484 and SNU601 cells transfected with miR-BART5-5p or miR-control; and EBV(+) SNU719 and YCCEL1 transfected with anti-miR-BART5-5p or miR-control. Expression levels were normalized to RNU6B. **e** PIAS3 mRNA levels by RT-PCR analysis. **f** Expression of PIAS3 by western blot analysis in EBV(–) SNU216, SNU484, and SNU601 cells transfected with miR-BART5-5p or miR-control; and in EBV(+) SNU719 and YCCEL1 cells transfected with anti-miR-BART5-5p or miR-control. Representative images (bottom) and quantification of PIAS3 expression by densitometry (bar graphs). **g** Luciferase reporter assay (upper bar graph) in HEK293T cells co-transfected with miR-BART5-5p and PIAS3 3'-UTR, or an empty vector (NC); and co-transfected with miR-control and PIAS3 3'-UTR, or empty vector (NC). For all graphs, data represent mean \pm SD of triplicate measurements. β -actin was used as a loading control. (Bottom) 6-mer sequence alignment of miR-BART5-5p and PIAS3 mRNA

miR-BART5-5p activates signal transducer and activator of transcription 3 (STAT3) by downregulating PIAS3

PIAS3 was named based on its initial characterization as a “protein inhibitor of activated STAT3” [31]. Therefore, we postulated that miR-BART5-5p-induced inhibition of PIAS3 may activate STAT3, which promotes its translocation to the nucleus. Consistent with this hypothesis, the functional binding site for STAT3 matches the promoter region of the hsa-miR-17–92 cluster (which includes hsa-miR-18a) [32], and hsa-miR-18a/b exhibits seed identity (nucleotides 2–7) with EBV miR-BART5-5p, according to informatics analysis (<https://www.mirbase.org>) (Fig. 1c).

To determine whether the inhibition of PIAS3 by miR-BART5-5p promotes the activation of STAT3, we evaluated the nuclear localization of STAT3 by fluorescence microscopy and western blot analysis of nuclear protein extracts, since activated STAT3 (phosphorylated STAT3) translocates to the nucleus, where STAT3 transcribes various genes [31]. In the SNU601 cells, which are EBV(–) cells that do not express miR-BART5-5p endogenously, we observed nuclear localization of STAT3 in the miR-BART5-5p-transfected cells, but not in the control-transfected cells (Fig. 3a). Using identically-treated cells, we confirmed these results by western blot analysis of nuclear protein extracts (Fig. 3b, images) and their quantification by densitometry (Fig. 3b, bar graphs).

Through western blot analysis, we assessed PIAS3, STAT3, and activated STAT3 (pSTAT3) protein levels in total cell extracts of SNU601 cells co-transfected with miR-BART5-5p and a PIAS3 expression plasmid/or empty vector; and in extracts of SNU601 cells co-transfected with a miR-control and a PIAS3 expression plasmid/or empty vector. We found that miR-BART5-5p enhanced pSTAT3 upregulation, and this pSTAT3 upregulation was offset by PIAS (Fig. 3c). miR-BART5-5p or PIAS3 had no effect on total STAT3 levels.

Conversely, we co-transfected YCCEL1 EBV (+) cells, which endogenously express miR-BART5-5p, with anti-miR-BART5-5p and a PIAS3-specific siRNA (siPIAS3)/or a scrambled control siRNA (siSCR), with siPIAS3 and a miR-control, or with siSCR and a miR-control. We collected total cell extracts and evaluated the expression of the aforementioned proteins by western blot analysis. We found that anti-miR-BART5-5p decreased endogenous levels of STAT3 activation, and this pSTAT3 downregulation was ablated by PIAS3 knockdown (Fig. 3d).

These results suggest that miR-BART5-5p activates STAT3 by downregulating PIAS3 in gastric carcinoma.

miR-BART5-5p upregulates PD-L1 in a STAT3-dependent manner

PD-L1—initially known as a crucial immune checkpoint molecule—transports antiapoptotic signals to cancer cells [33]. The *PD-L1* gene promoter contains specific sequences (response elements) that bind to STAT3 [34, 35]. Accordingly, we inferred that PD-L1 was downstream in the miR-BART5-5p/PIAS3/pSTAT3 axis. miR-BART5-5p transfection significantly enhanced the expression of PD-L1 in SNU601 cells compared to control-transfected cells ($P=0.007$). Conversely, anti-miR-BART5-5p transfection significantly reduced the expression of PD-L1 in YCCEL1 EBV(+) cells compared to control-transfected cells ($P=0.034$) (Fig. 4a).

To assess whether STAT3 may control the transcription of *PD-L1* in gastric carcinoma, we transfected SNU601 EBV(–) cells with an miR-control or miR-BART5-5p, and treated them with S3I-201 (a STAT3 inhibitor) or dimethylsulfoxide (DMSO). As a result, miR-BART5-5p upregulated PD-L1 and pSTAT3, and this miR-BART5-5p-induced PD-L1 upregulation was abrogated by STAT3 inhibition (Fig. 4b). Conversely, in YCCEL1 EBV(+) cells, anti-miR-BART5-5p downregulated PD-L1 and pSTAT3, and this PD-L1 downregulation was restored by transfection with a STAT3 expression plasmid (Fig. 4c). These results indicate that miR-BART5-5p enhances PD-L1 expression by activating STAT3 in gastric carcinoma cells.

PD-L1 knockdown enhances apoptosis in miR-BART5-5p-transfected cells

To determine whether apoptosis may be modified by miR-BART5-5p-PIAS3/pSTAT3/PD-L1 axis control, we abolished PD-L1 upregulation in miR-BART5-5p-transfected SNU601 cells by treatment with a PD-L1-specific siRNA (siPD-L1) (Fig. 5a). Using these cells, we evaluated the effect of PD-L1 on serum deprivation-induced apoptosis by flow cytometry. After 48 h of serum deprivation, the miR-BART5-5p-transfected SNU601 cells treated with siPD-L1 showed significantly increased apoptosis compared to cells treated with the scrambled siRNA (siSCR) ($P=0.002$) (Fig. 5b). Furthermore, the rate of cell proliferation was lowered, and the invasion capacity and migration of miR-BART5-5p-transfected SNU601 cells treated with siPD-L1 were reduced compared to those of cells treated with scrambled siRNA ($P<0.001$) (Fig. 5c–e).

Since transfecting miR-BART5-5p into SNU601 and SNU216 cells (SNU601 miR-BART5-5p and SNU216 miR-BART5-5p, respectively) had no effect on apoptosis compared to the miR-control-transfected cells after 48 h (S4A Fig), we extended the experiment to 96 h. However, even after 96 h of serum deprivation, there was no

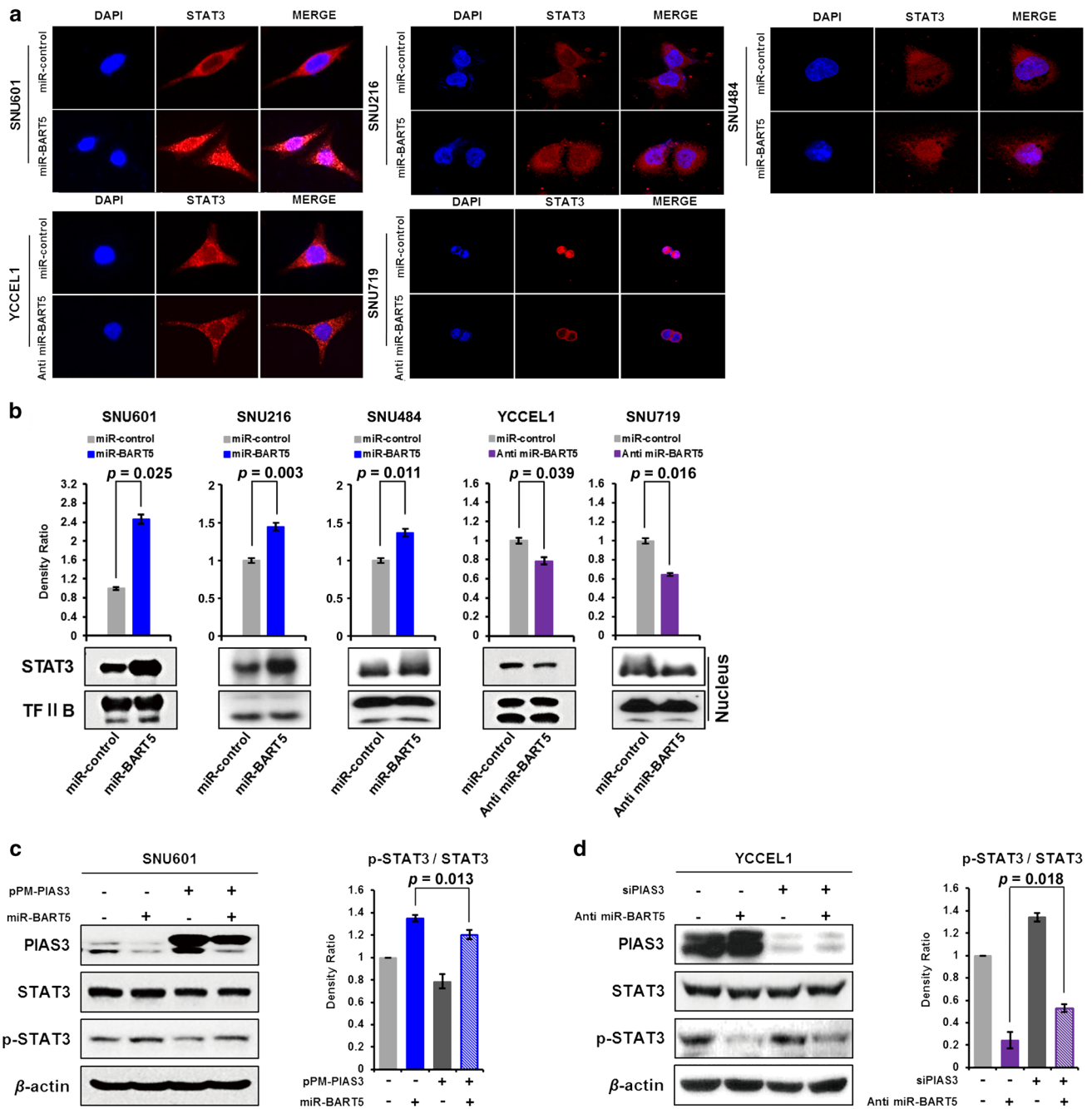


Fig. 3 miR-BART5-5p induces nuclear translocation of STAT3 and upregulates pSTAT3 in a PIAS3-downregulation-dependent manner. **a** STAT3 and DAPI expression by immunofluorescence in SNU601, SNU216, and SNU484 cells transfected with miR-BART5-5p or miR-control; and YCCEL1 and SNU719 cells transfected with anti-miR-BART5-5p or miR-control; (STAT3: red; nuclei/DAPI: blue). **b** Expression of STAT3 by western blot analysis in nuclear extracts of SNU601, SNU216, and SNU484 cells transfected with miR-BART5-5p or miR-control; and YCCEL1 and SNU719 cells transfected with anti-miR-BART5-5p or miR-control. Representative images (bottom) and quantification of STAT3 by densitometry (bar graphs). **c** Expression of PIAS3, STAT3, and pSTAT3 by western blot analysis in total cellular extracts of SNU601 cells transfected with empty vector and miR-control, empty vector and miR-BART5-5p, PIAS3

expression plasmid (pPM-PIAS3) and miR-control, or miR-BART5-5p and pPM-PIAS3 (representative images, left); quantification of the ratio of pSTAT3/STAT3 by densitometry (bar graph). **d** Expression of PIAS3, STAT3, and pSTAT3 in total cellular extracts by western blot analysis of YCCEL1 cells transfected with siRNA scrambled control (siSCR) and miR-control, anti-miR-BART5-5p and scrambled siSCR, PIAS3-specific siRNA (siPIAS3) and miR-control, or with siPIAS3 and anti-miR-BART5-5p (representative images, left); quantification of the ratio of pSTAT3/STAT3 by densitometry (bar graph). Transcription factor IIB (TF II B) was used as the loading control for nuclear extracts, and β -actin as the loading control for total cellular extracts. For all graphs, data represent mean \pm SD of triplicate measurements

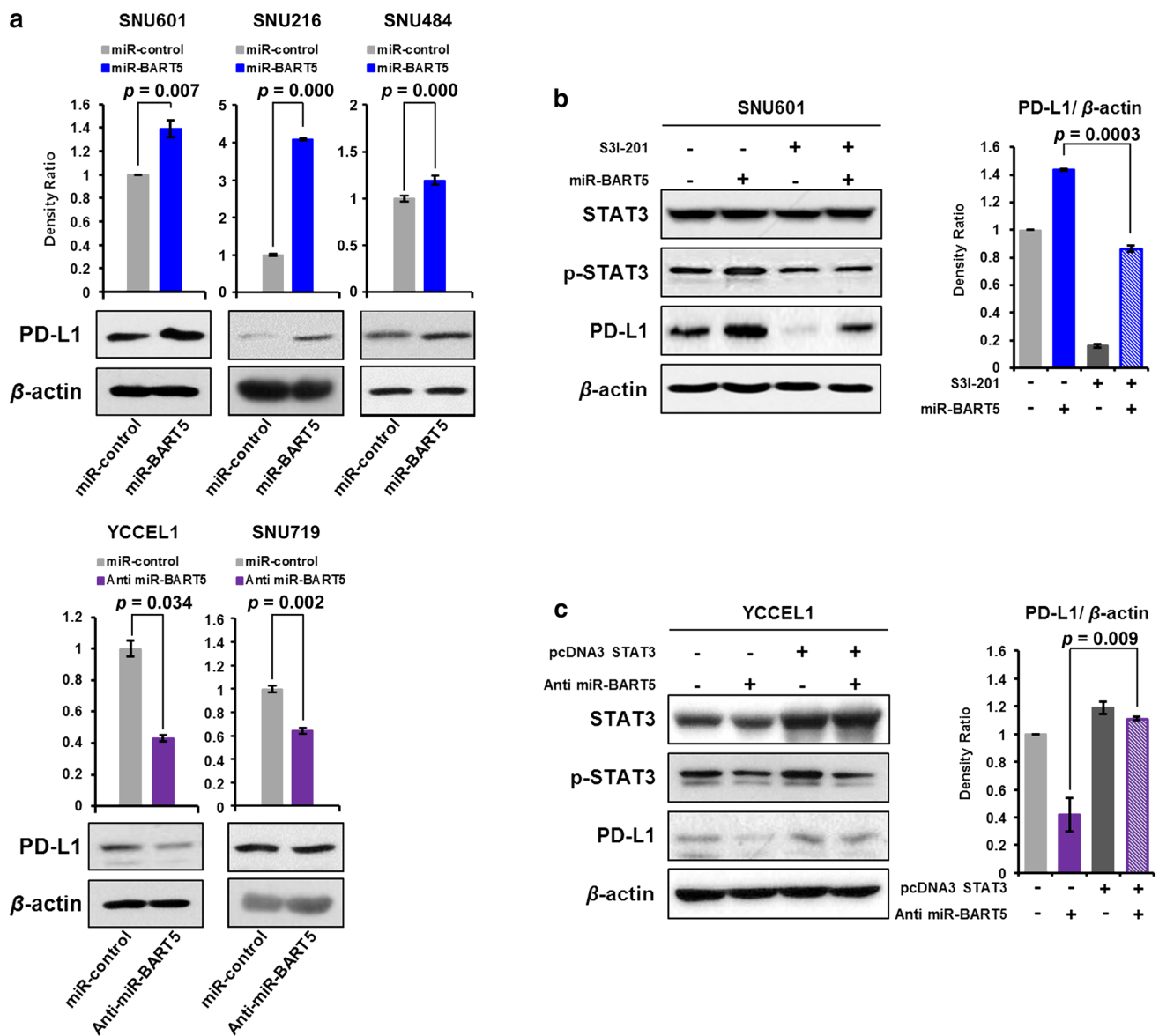


Fig. 4 miR-BART5-5p upregulates PD-L1 in a pSTAT3-dependent manner. **a** Expression of PD-L1 by western blot analysis in SNU601, SNU216, and SNU484 cells transfected with miR-BART5-5p or miR-control (upper column); and in YCCEL1 and SNU719 cells transfected with anti-miR-BART5-5p or miR-control (lower column). **b** Expression of STAT3, pSTAT3, and PD-L1 by western blot analysis in SNU601 cells transfected with dimethyl sulfoxide (DMSO) and miRNA-control, DMSO and miR-BART5-5p, STAT3 inhibitor (S3I-201) and miRNA-control, or miR-BART5-5p and S3I-201 (representative images, left); quantification of PD-L1, normalized to β -actin by densitometry (bar graph). **c** Expression of STAT3, pSTAT3, and PD-L1 by western blot analysis in YCCEL1 cells transfected with empty vector and miR-control, anti-miR-BART5-5p and empty vector, STAT3 expression plasmid (pcDNA3 STAT3) and miR-control, or pcDNA3 STAT3 and miR-BART5-5p (representative images, left); quantification of PD-L1 normalized to β -actin by densitometry (bar graph). β -actin was used as a loading control throughout. For all graphs, data represent mean \pm SD of triplicate measurements

difference in apoptosis between the cells transfected with miR-BART5-5p and the control miR-transfected cells (S4A Fig). In addition, miR-BART5-5p did not affect the rate of cell proliferation (S4B Fig), invasion capacity (S4C Fig), and migration (S4D Fig).

Tumoral PD-L1 expression is associated with adverse clinical outcomes in patients with EBV-associated gastric carcinoma

Since we found that PD-L1 inhibited apoptosis, we hypothesized that the expression of PD-L1 by tumor cells may be

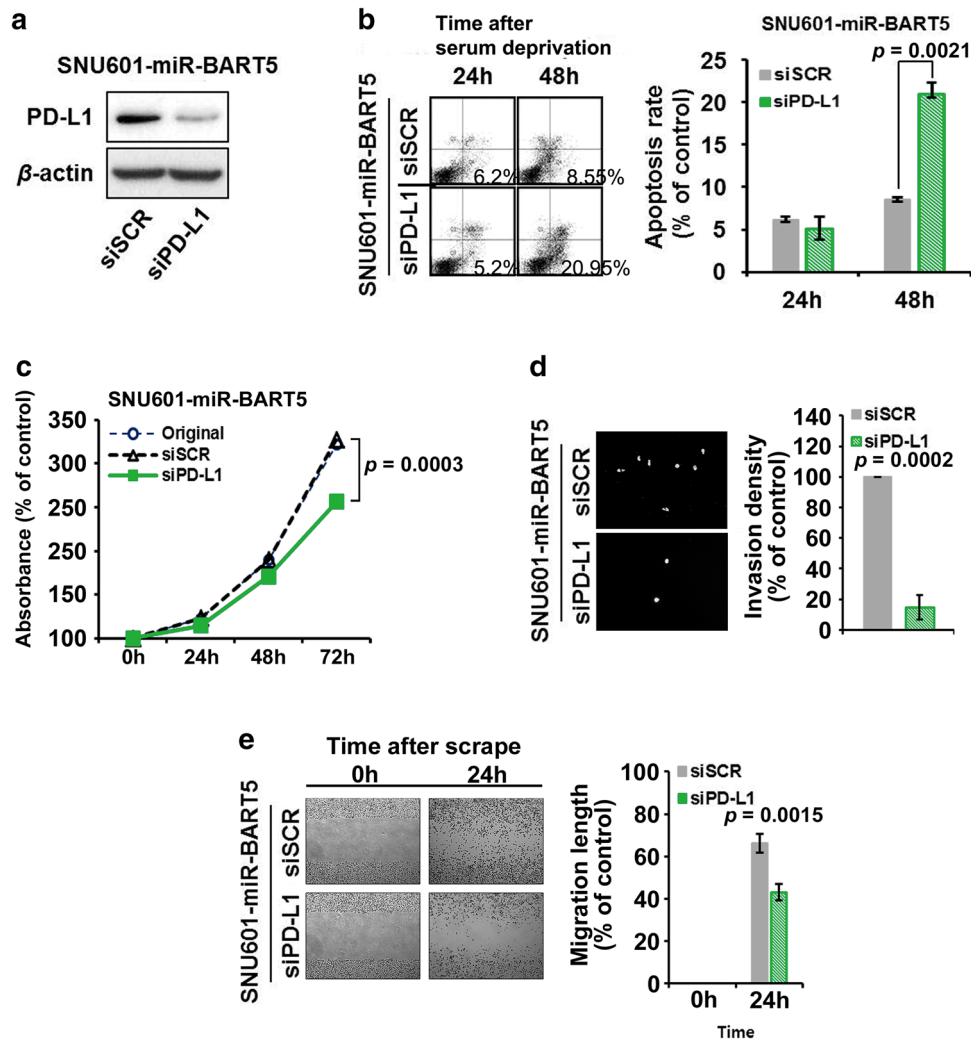


Fig. 5 PD-L1 knockdown enhances apoptosis and reduces the cell proliferation rate, invasion capacity, and migration of miR-BART5-transfected SNU601 cells. **a** Expression of PD-L1 by western blot analysis in miR-BART5-5p-transfected SNU601 cells treated with scrambled siRNA control (siSCR) or PD-L1-specific siRNA (siPD-L1). **b** Serum deprivation-induced apoptosis in miR-BART5-5p-transfected SNU601 cells, transfected with siPD-L1 or siSCR. The percentage of apoptotic cells was determined by annexin V (+)/propidium iodide (-) cells (bottom right quadrant of image). Quantification of the percent of apoptotic cells after 24 and 48 h of serum deprivation. Data represent mean \pm SD of triplicate measurements. **c** Evaluation of cell proliferation in three cell lines using the WST-1 assay; miR-BART5-5p-transfected SNU601 cells treated with siPD-

L1, miR-BART5-5p-transfected SNU601 cells treated with siSCR, and original SNU601 cells. **d** Matrix invasion assay. Cells that infiltrated through invasion chambers were photographed using a fluorescence microscope (representative images, left) and their invasion density is indicated in a bar graph. **e** Cell migration was assessed by a wound healing assay. Representative images of miR-BART5-5p-transfected SNU601 cells treated with siPD-L1, and miR-BART5-5p-transfected SNU601 cells treated with siSCR at the indicated time points after wound scratching (left). The percentage of wound healing was calculated as 0-, 24-h distances of wound/0-h distance (bar graph). Distance was measured in at least three randomly-selected fields. For all graphs, data represent mean \pm SD of triplicate measurements

linked to the survival of patients with EBV-associated gastric carcinomas. To this end, we evaluated tissues samples from 103 patients with EBV-associated gastric carcinoma obtained during surgical resection (Fig. 6a; Supplemental Table 1). Immunohistochemically, 94% (97/103) of the tumor tissue samples were PIAS3 negative, 40% (41/103) were pSTAT positive, and 50% (51/103) were PD-L1

positive (Fig. 6b–e). There was no statistically significant correlation among the expression of these three proteins in gastric carcinoma tissues. For the clinical outcomes of patients with EBV-associated gastric carcinoma, those with tumoral expression of PD-L1 had a significantly lower overall survival rate than patients whose tumors were negative for PD-L1 ($P = 0.049$) (Fig. 6f).

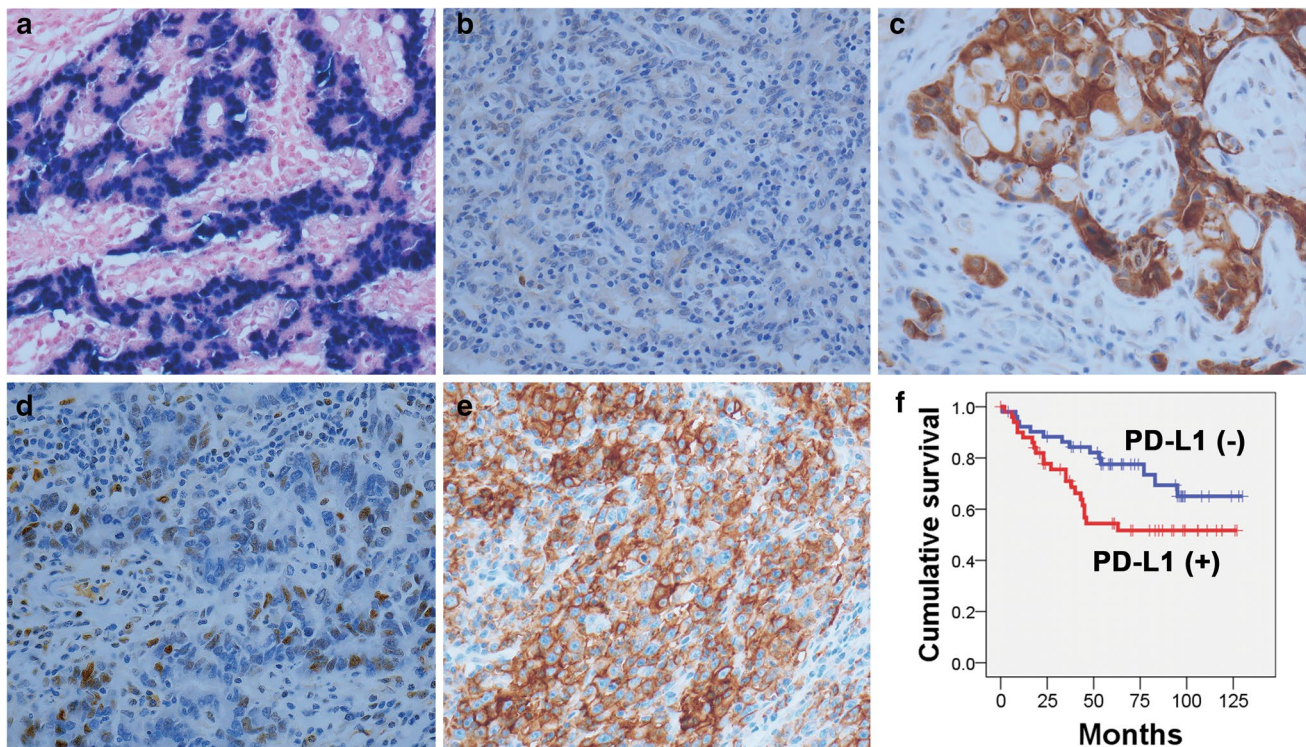


Fig. 6 Histopathological features of EBV-associated gastric carcinoma tissues and clinical outcome of patients with EBV-associated gastric carcinoma, \pm PD-L1. **a** Representative image of nuclear expression of Epstein–Barr virus-encoded small RNAs by in situ hybridization (black/dark blue staining). Representative immunohistochemical analysis of **b** PIAS3 loss, **c** cytoplasmic and nuclear

PIAS3 expression, **d** nuclear pSTAT3 expression, and **e** membrane-bound PD-L1 expression in tumor cells. **f** Kaplan–Meier plot of the comparative overall survival of 103 patients with EBV-associated gastric carcinomas based on PD-L1 status. Tumoral PD-L1 (+) group shows a lower survival rate than tumoral PD-L1 (–) group ($P=0.049$)

Discussion

The present study suggests that EBV-encoded miR-BART5-5p may inhibit apoptosis and promote immune evasion, contributing to the progression of EBV-associated gastric carcinomas. We demonstrated that miR-BART5-5p induced PD-L1 upregulation. Apoptosis increased, while cell proliferation, invasion, and migration decreased when PD-L1 upregulation was abrogated by PD-L1-specific siRNAs in miR-BART5-5p-transfected cells, characterizing PD-L1 as an antiapoptotic factor and a tumor growth-promoting factor. This is consistent with prior studies which showed that PD-L1 can relay antiapoptotic signaling to cancer cells, acting as a transmembrane receptor [33]. In addition, PD-L1 knockdown led to the suppression of cell proliferation, invasion, and migration [36]. To our knowledge, this is the first documentation of PD-L1 upregulation by an EBV-encoded miRNA. Besides, miR-BART5-5p-mediated PD-L1 upregulation may assist EBV in the evasion of immune surveillance. Accumulating evidence indicates that upregulation of PD-L1 is crucial for immune escape. The PD-1/PD-L1 (receptor/ligand) interaction acts like an immune brake (i.e., it allows PD-L1 expressing cells to evade immune

surveillance) [37]. In other words, when cancer cells that aberrantly express PD-L1 bind to PD-1-expressing T cells, they hijack a mechanism that normally controls the autoimmune response and protect themselves from the T cell-mediated killing effect [38]. In this study, we observed that the PD-L1(+) patient group had a lower rate of overall survival than the PD-L1(–) group of patients with EBV-associated gastric carcinomas. This study of 103 patients with EBV(+) gastric carcinomas belongs to one of the largest series of single institute studies dealing with the prognosis of EBV-associated gastric carcinoma patients [39]. Our data connote that miR-BART5-5p-mediated PD-L1 upregulation may enhance cancer progression by inhibiting apoptosis and promoting immune escape. Such finding suggests that PD-1/PD-L1 immune inhibitor therapy may benefit the PD-L1(+) group. In addition to miR-BART5-5p activity, PD-L1 upregulation may occur via multiple mechanisms in EBV-associated gastric carcinomas, including the amplification of chromosomal region 9p24.1, which includes the *PD-L1* gene [5], and mutations in the 3'-UTR of PD-L1 [40]. Furthermore, in this tissue context, EBV-associated gastric carcinomas are characterized by heavy lymphocyte infiltration with cells, such as CD8⁺ cytotoxic T lymphocytes [41]. CD8⁺ cells

secrete interferon- γ , and interferon- γ extrinsically induces the upregulation of PD-L1 on the cancer cell surface [42].

The present study indicates that miR-BART5/PIAS3/pSTAT3/PD-L1 axis control works in EBV-associated gastric carcinoma via viral miRNA-induced human cellular signaling activation. In this study, we found that miR-BART5-5p directly targeted the 3'-UTR of PIAS3, down-regulating PIAS3 protein levels, which activated STAT3 and enhanced the expression of PD-L1. To our knowledge, this study provides the first evidence that a viral miRNA directly targets PIAS3. PIAS3 interrupts the phosphorylation of STAT3 via PIAS3 binding to the STAT3 DNA binding domain, thereby inhibiting STAT3 activation and suppressing the expression of STAT3-mediated proteins [31, 35, 43]. Phosphorylated STAT3 proteins form dimers, and STAT3 dimers translocate to the cell nucleus, where they function as transcriptional activators [44, 45]. STAT3 regulates many genes including *PD-L1* [45–47], and induces CD4+ Th 17 cell differentiation [48]. Therefore, “PIAS3 down regulation/STAT3 upregulation/PD-L1 upregulation” may play a role in the suppression of both innate and adaptive immunity [43].

The miR-BART5/PD-L1 axis seems to be irrelevant to hsa-miR-18a-5p, despite seed sequence homology between miR-BART5-5p and hsa-miR-18a-5p. When transfecting miR-BART5-5p into three EBV(–) gastric carcinoma cell lines, and anti-miR-BART5-5p into two EBV(+) gastric carcinoma cell lines, there was no significant change in the level of hsa-miR-18a-5p (S5A Fig). Additionally, hsa-miR-18a-5p affected the level of PD-L1 in three out of five cell lines, which was irrespective of EBV status (S5B Fig). In keeping with recent reports, we observed that many hsa-miRNAs were lowered in EBV(+) cells compared to EBV(–) cells. EBV-infection could provoke striking alteration in the cellular miRNA repertoire; mainly, it downregulates the tumor suppressor hsa-miRNAs (anti-oncomiRs), and upregulates oncomiRs, and could thus contribute to carcinogenesis [11, 49, 50]. Further studies will warrant elucidating the regulatory mechanisms between hsa-miRNAs and ebv-miRNAs. With regard to ebv-miRNAs profiling in the present study, miR-BART22 was the highest expressed in EBV(+) cells, and miR-BART22 did not affect PD-L1 level in five gastric carcinoma cell lines (S5C Fig). Compared to previous works, miR-BART22 was highly expressed in EBV-associated gastric carcinomas from The Cancer Genome Atlas (TCGA) project and other reports [5, 51–53]. On the other hand, Shinozaki-Ushiku et al. reported that expression of miR-BART22 was low, and that of miR-BART7-3p was highest in EBV(+) gastric carcinoma tissues and EBV(+) SNU719 cells [54], whereas Tsai et al. stated that miR-BART18-5p expression was the highest in EBV(+) SNU719 cells [55]. In our microRNA data, miR-BART7-3p was the second most highly expressed in gastric carcinoma tissues and the fourth in EBV(+) YCCEL1 cells, whereas

expression of miR-BART18-5p was the third in EBV(+) cells. The reasons for this discrepancy largely lie in the use of different detection methods and the different latency types [54]. Furthermore, we addressed additional possible reasons: time-dependent dynamic heterogeneity of ebv-miRNAs levels according to the cancer progression, cancer type- or cell line-specific miRNAs characteristics, etc.

This study has some inherent limitations. Our findings were obtained in miR-BART5-5p mimic-transfected cells, and not in stably transfected cells. In our experience, cells stably transfected with the pTRIPZ-miR-BART5 plasmid yielded very low miR-BART5-5p expression levels: up to 222-fold less than in EBV(+) gastric carcinoma cell lines (Fig. S1), even if we accept that the expression levels of EBV miRNAs have varied by nearly 50-fold among six types of EBV-infected cell lines [9]. Instead, we adjusted the amount of miR-BART5-5p mimic transfection, to reflect physiological levels of expression and lessen transfection stress. We also noticed that transfection with an excessive amount (100 nM) of miR-BART5-5p mimic reduced cell proliferation and increased apoptosis (data not shown), probably due to transfection stress, which may lead to the misconception that EBV-miRNAs might act as anticancer components. To address another issue, apoptosis increased with statistical significance when miR-BART5-5p-mediated PD-L1 upregulation was ablated by PD-L1-specific siRNA in miR-BART5-5p-transfected cells. This implies that PD-L1 inhibits apoptosis. However, cells initially transfected with miR-BART5 showed minimally decreased apoptosis (without statistical significance) compared to control cells. To explain these findings, we conjecture that PD-L1 increase by a single viral miRNA may be insufficient to cause a statistically significant effect on apoptosis. Indeed, the accumulating assistance of multiple miRNAs engenders synergistic effects [13]; a cluster of EBV miRNAs (i.e., miR-BART cluster 1 or cluster 2) acts together to affect biological activities, such as cell growth in the mouse model of nasopharyngeal carcinoma and gastric carcinoma [56], antiapoptosis in gastric carcinoma cells [57], migration in epithelial cells [58], and B cell transformation [59]. Lastly, we could not find statistical correlations among the immunohistochemical results of PIAS3, STAT3, and PD-L1 in EBV-associated gastric carcinoma tissues. We suggest that the lack of correlation may occur, because the expression of these cancer-related proteins may be affected not only by the cancer cell itself, but also by the complex tumor microenvironment.

In summary, miR-BART5-5p directly targets PIAS3, and induces PD-L1 upregulation through miR-BART5/PIAS3/pSTAT3/PD-L1 axis control, where a viral miRNA cooperates with human cellular signaling (see model in Fig. 7). miR-BART5-mediated PD-L1 upregulation may be involved in inhibiting apoptosis and assisting immune evasion, leading to cancer progression, rather than initiating

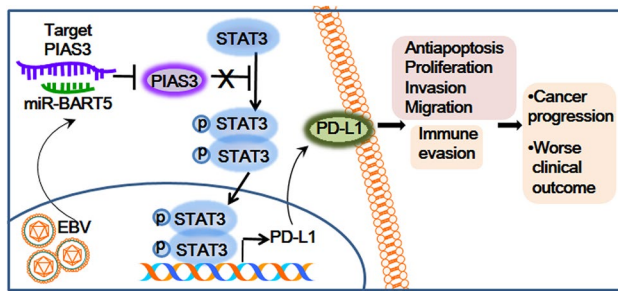


Fig. 7 Schematic of miR-BART5-5p-mediated PIAS3/pSTAT3/PD-L1 axis control in EBV-associated gastric carcinoma. This model illustrates a possible mechanism by which EBV-encoded miR-BART5-5p may contribute to the progression of EBV-associated gastric carcinoma. miR-BART5-5p directly targets PIAS3, downregulating PIAS3 protein levels, and subsequently activating STAT3. Activated STAT3 (phosphorylated STAT3) translocates to the nucleus, where it promotes the transcription of the *PD-L1* gene, upregulating PD-L1 levels. PD-L1 promotes gastric carcinoma progression and worse clinical outcomes by inhibiting tumor cell apoptosis and facilitating immune evasion

transformation of gastric epithelial cells. This concept is consistent with our finding that the PD-L1(+) group had worse clinical outcomes than the PD-L1(−) group of patients with EBV-associated gastric carcinoma, thereby predicting a positive clinical response to PD-1/PD-L1 immune checkpoint inhibitor therapy in the PD-L1(+) group. The present study, where miR-BART5-5p functions as an oncogenic miRNA, further supports the characterization of EBV as an oncogenic virus, in light of the exceedingly limited expression of viral proteins (four of EBER, EBNA1, LMP2A, and BART1) [2] in EBV-associated gastric carcinomas.

Acknowledgements This study was supported by the Basic Science Research Program through The National Research Foundation of Korea (NRF), funded by the Ministry of Education under award number 2016R1D1A1B01010316 (to MSC). The funders had no role in study design, data collection and interpretation or the decision to submit the study for publication. The authors are very thankful to Professor Bryan R. Cullen (Duke University, NC, USA) for sharing the pTRIPZ-miR-BART5 plasmid. The authors also thank Macrogen (Seoul, Republic of Korea) for microRNA microarray analysis, and Jin Hee Han and Cheo Ho Im for performing the immunohistochemistry and in situ hybridization experiments.

Compliance with ethical standards

Conflict of interest The authors have declared that no conflict of interests exists.

Ethical approval This study protocol was reviewed and approved by the Institutional Review Board of the Seoul National University Boramae Hospital under conditions of anonymity (IRB No. 20140204/26-2014-13/022). All human tissue specimens were obtained during diagnostic and therapeutic surgery. This study was performed using the stored paraffin blocks containing tissue samples after the pathologic diagnosis, and all of the samples were anonymized before the study.

Informed consent Complying with the Bioethics and Safety act fully revised and effective February 1, 2013 in Republic of Korea, participants undergone surgery after February 1, 2013 are supposed to provide the informed consent for the study using paraffin block-embedded tissues. In this study, the patients undergone surgery before February 1, 2013 did not submit the informed consent according to the Bioethics and Safety act of the time.

References

1. Young LS, Rickinson AB. Epstein–Barr virus: 40 years on. *Nat Rev Cancer*. 2004;4:757–68.
2. Longnecker RM, Kieff E, Cohen JI. Epstein–Barr virus. In: Knipe DM, Howley PM, editors. *Fields virology*. 6th ed. Philadelphia: Lippincott-Williams and Wilkins; 2013. p. 1898–1959.
3. Jung KW, Won YJ, Kong HJ, Lee ES. Cancer statistics in Korea: incidence, mortality, survival, and prevalence in 2015. *Cancer Res Treat*. 2018;50:303–16.
4. Chang MS, Kim DH, Roh JK, Middeldorp JM, Kim YS, Kim S, et al. Epstein–Barr virus-encoded BART1 promotes proliferation of gastric carcinoma cells through regulation of NF- κ B. *J Virol*. 2013;87:10515–23.
5. Cancer Genome Atlas Research Network. Comprehensive molecular characterization of gastric adenocarcinoma. *Nature*. 2014;513:202–9.
6. Cristescu R, Lee J, Nebozhyn M, Kim KM, Ting JC, Wong SS, et al. Molecular analysis of gastric cancer identifies subtypes associated with distinct clinical outcomes. *Nat Med*. 2015;21:449–56.
7. Strong MJ, Xu G, Coco J, Baribault C, Vinay DS, Lacey MR, et al. Differences in gastric carcinoma microenvironment stratify according to EBV infection intensity: implications for possible immune adjuvant therapy. *PLoS Pathog*. 2013;9:e1003341.
8. Gu L, Chen M, Guo D, Zhu H, Zhang W, Pan J, et al. PD-L1 and gastric cancer prognosis: a systematic review and meta-analysis. *PLoS ONE*. 2017;12:e0182692.
9. Pratt ZL, Kuzembayeva M, Sengupta S, Sugden B. The microRNAs of Epstein–Barr virus are expressed at dramatically differing levels among cell lines. *Virology*. 2009;386:387–97.
10. Pfeffer S, Zavolan M, Grässer FA, Chien M, Russo JJ, Ju J, et al. Identification of virus-encoded microRNAs. *Science*. 2004;304:734–6.
11. Marquitz AR, Mathur A, Chugh PE, Dittmer DP, Raab-Traub N. Expression profile of microRNAs in Epstein–Barr virus-infected AGS gastric carcinoma cells. *J Virol*. 2014;88:1389–93.
12. Kim DN, Chae HS, Oh ST, Kang JH, Park CH, Park WS, et al. Expression of viral microRNAs in Epstein–Barr virus-associated gastric carcinoma. *J Virol*. 2007;81:1033–6.
13. Flór TB, Blom B. Pathogens use and abuse microRNAs to deceive the immune system. *Int J Mol Sci*. 2016;17:538.
14. Choy EY, Siu KL, Kok KH, Lung RW, Tsang CM, To KF, et al. An Epstein–Barr virus-encoded microRNA targets PUMA to promote host cell survival. *J Exp Med*. 2008;205:2551–600.
15. Zheng X, Wang J, Wei L, Peng Q, Gao Y, Fu Y, et al. Epstein–Barr virus microRNA miR-BART5-3p inhibits p53 expression. *J Virol*. 2018;92:e01022–18.
16. Kim H, Choi H, Lee SK. Epstein–Barr virus miR-BART20-5p regulates cell proliferation and apoptosis by targeting BAD. *Cancer Lett*. 2015;356:733–42.
17. Choi H, Lee H, Kim SR, Gho YS, Lee SK. Epstein–Barr virus-encoded microRNA BART15-3p promotes cell apoptosis partially by targeting BRUCE. *J Virol*. 2013;87:8135–44.
18. Cai L, Ye Y, Jiang Q, Chen Y, Lyu X, Li Z, et al. Epstein–Barr virus-encoded microRNA BART1 induces tumour metastasis

- by regulating PTEN-dependent pathways in nasopharyngeal carcinoma. *Nat Commun.* 2015;6:7353.
19. Lei T, Yuen KS, Xu R, Tsao SW, Chen H, Li M, et al. Targeting of DICE1 tumor suppressor by Epstein–Barr virus-encoded miR-BART3 microRNA in nasopharyngeal carcinoma. *Int J Cancer.* 2013;133:79–877.
 20. Lu Y, Qin Z, Wang J, Zheng X, Lu J, Zhang X, et al. Epstein–Barr Virus miR-BART6-3p Inhibits the RIG-I Pathway. *J Innate Immun.* 2017;9:574–86.
 21. Lin C, Zong J, Lin W, Wang M, Xu Y, Zhou R, et al. EBV-miR-BART8-3p induces epithelial-mesenchymal transition and promotes metastasis of nasopharyngeal carcinoma cells through activating NF- κ B and Erk1/2 pathways. *J Exp Clin Cancer Res.* 2018;37:283.
 22. Hsu CY, Yi YH, Chang KP, Chang YS, Chen SJ, Chen HC. The Epstein–Barr virus-encoded microRNA MiR-BART9 promotes tumor metastasis by targeting E-cadherin in nasopharyngeal carcinoma. *PLoS Pathog.* 2014;10:e1003974.
 23. Yan Q, Zeng Z, Gong Z, Zhang W, Li X, He B, et al. EBV-miR-BART10-3p facilitates epithelial-mesenchymal transition and promotes metastasis of nasopharyngeal carcinoma by targeting BTRC. *Oncotarget.* 2015;6:41766–82.
 24. Kim DH, Chang MS, Yoon CJ, Middeldorp JM, Martinez OM, Byeon SJ, et al. Epstein–Barr virus BARF1-induced NF κ B/miR-146a/SMAD4 alterations in stomach cancer cells. *Oncotarget.* 2016;7:82213–27.
 25. Bolstad BM, Irizarry RA, Astrand M, Speed TP. A comparison of normalization methods for high density oligonucleotide array data based on variance and bias. *Bioinformatics.* 2003;19:185–93.
 26. Jeong JY, Woo JH, Kim YS, Choi S, Lee SO, Kil SR, et al. Nuclear factor-kappa B inhibition reduces markedly cell proliferation in Epstein–Barr virus-infected stomach cancer, but affects variably in Epstein–Barr virus-negative stomach cancer. *Cancer Investig.* 2010;28:113–9.
 27. Kluge A, Dabir S, Vlassenbroeck I, Eisenberg R, Dowlati A. Protein inhibitor of activated STAT3 expression in lung cancer. *Mol Oncol.* 2011;5:256–64.
 28. Chen SJ, Chen GH, Chen YH, Liu CY, Chang KP, Chang YS, et al. Characterization of Epstein–Barr virus miRNAome in nasopharyngeal carcinoma by deep sequencing. *PLoS ONE.* 2010;5:e12745.
 29. Babu SG, Ponia SS, Kumar D, Saxena S. Cellular oncomiR orthologue in EBV oncogenesis. *Comput Biol Med.* 2011;41:891–8.
 30. Wu W, Takanashi M, Borjigin N, Ohno SI, Fujita K, Hoshino S, et al. MicroRNA-18a modulates STAT3 activity through negative regulation of PIAS3 during gastric adenocarcinogenesis. *Br J Cancer.* 2013;108:653–61.
 31. Chung CD, Liao J, Liu B, Rao X, Jay P, Berta P, et al. Specific inhibition of Stat3 signal transduction by PIAS3. *Science.* 1997;278:1803–5.
 32. He L, Thomson JM, Hemann MT, Hernando-Monge E, Mu D, Goodson S, et al. A microRNA polycistron as a potential human oncogene. *Nature.* 2005;435:828–33.
 33. Azuma T, Yao S, Zhu G, Flies AS, Slier SJ, Chen L, et al. B7-H1 is a ubiquitous antiapoptotic receptor on cancer cells. *Blood.* 2008;111:3635–43.
 34. Marzec M, Zhang Q, Goradia A, Raghunath PN, Liu X, Paessler M, et al. Oncogenic kinase NPM/ALK induces through STAT3 expression of immunosuppressive protein CD274 (PD-L1, B7-H1). *Proc Natl Acad Sci USA.* 2008;105:20852–7.
 35. Prestipino A, Zeiser R. Clinical implications of tumor-intrinsic mechanisms regulating PD-L1. *Sci Transl Med.* 2019;11:eaav4810.
 36. Li J, Chen L, Xiong Y, Zheng X, Xie Q, Zhou Q, et al. Knockdown of PD-L1 in human gastric cancer cells inhibits tumor progression and improves the cytotoxic sensitivity to CIK therapy. *Cell Physiol Biochem.* 2017;41:907–20.
 37. Pardoll DM. The blockade of immune checkpoints in cancer immunotherapy. *Nat Rev Cancer.* 2012;12:252–64.
 38. Ying L, Yan F, Meng Q, Yu L, Yuan X, Gantier MP, et al. PD-L1 expression is a prognostic factor in subgroups of gastric cancer patients stratified according to their levels of CD8 and FOXP3 immune markers. *Oncoimmunology.* 2018;7:e1433520.
 39. Liu X, Liu J, Qiu H, Kong P, Chen S, Li W, et al. Prognostic significance of Epstein–Barr virus infection in gastric cancer: a meta-analysis. *BMC Cancer.* 2015;15:782.
 40. Wang W, Sun J, Li F, Li R, Gu Y, Liu C, et al. A frequent somatic mutation in CD274 3-UTR leads to protein over-expression in gastric cancer by disrupting miR-570 binding. *Hum Mutat.* 2012;33:480–4.
 41. Kawazoe A, Kuwata T, Kuboki Y, Shitara K, Nagatsuma AK, Aizawa M, et al. Clinicopathological features of programmed death ligand 1 expression with tumor-infiltrating lymphocyte, mismatch repair, and Epstein–Barr virus status in a large cohort of gastric cancer patients. *Gastric Cancer.* 2017;20:407–15.
 42. Zou W, Chen L. Inhibitory B7-family molecules in the tumour microenvironment. *Nat Rev Immunol.* 2008;8:467–77.
 43. Yagil Z, Nechushtan H, Kay G, Yang CM, Kemeny DM, Razin E. The enigma of the role of protein inhibitor of activated STAT3 (PIAS3) in the immune response. *Trends Immunol.* 2010;31:199–204.
 44. Bromberg J, Darnell JE Jr. The role of STATs in transcriptional control and their impact on cellular function. *Oncogene.* 2000;19:2468–73.
 45. Yu H, Lee H, Hermann A, Buettner R, Jove R. Revisiting STAT3 signalling in cancer: new and unexpected biological functions. *Nat Rev Cancer.* 2014;14:736–46.
 46. Sun C, Mezzadra R, Schumacher TN. Regulation and function of the PD-L1 checkpoint. *Immunity.* 2018;48:434–52.
 47. Zerdes I, Matikas A, Bergh J, Rassidakis GZ, Foukakis T. Genetic, transcriptional and post-translational regulation of the programmed death protein ligand 1 in cancer: biology and clinical correlations. *Oncogene.* 2018;37:4639–61.
 48. Yang XO, Panopoulos AD, Nurieva R, Chang SH, Wang D, Watowich SS, et al. STAT3 regulates cytokine-mediated generation of inflammatory helper T cells. *J Biol Chem.* 2007;282:9358–63.
 49. Skalsky RL. Analysis of viral and cellular microRNAs in EBV-infected cells. *Methods Mol Biol.* 2017;1532:133–46.
 50. Kaneda A, Matsusaka K, Aburatani H, Fukayama M. Epstein–Barr virus infection as an epigenetic driver of tumorigenesis. *Cancer Res.* 2012;72:3445–500.
 51. Pandya D, Mariani M, He S, Andreoli M, Spennato M, Dowell-Martino C, et al. Epstein–Barr virus microRNA expression increases aggressiveness of solid malignancies. *PLoS ONE.* 2015;10:e0136058.
 52. Jing JJ, Wang ZY, Li H, Sun LP, Yuan Y. Key elements involved in Epstein–Barr virus-associated gastric cancer and their network regulation. *Cancer Cell Int.* 2018;18:146.
 53. Qiu J, Cosmopoulos K, Pegtel M, Hopmans E, Murray P, Middeldorp J, et al. A novel persistence associated EBV miRNA expression profile is disrupted in neoplasia. *PLoS Pathog.* 2011;7:e1002193.
 54. Shinozaki-Ushiku A, Kunita A, Isogai M, Hibiya T, Ushiku T, Takada K, et al. Profiling of virus-encoded microRNAs in Epstein–Barr virus-associated gastric carcinoma and their roles in gastric carcinogenesis. *J Virol.* 2015;89:5581–91.
 55. Tsai CY, Liu YY, Liu KH, Hsu JT, Chen TS, Chiu CT, et al. Comprehensive profiling of virus microRNAs of Epstein–Barr virus-associated gastric carcinoma: highlighting the interactions of ebv-Bart9 and host tumor cells. *J Gastroenterol Hepatol.* 2017;32:82–91.

56. Qiu J, Smith P, Leahy L, Thorley-Lawson DA. The Epstein–Barr virus encoded BART miRNAs potentiate tumor growth in vivo. *PLoS Pathog.* 2015;11:e1004561.
57. Kang D, Skalsky RL, Cullen BR. EBV BART microRNAs target multiple pro-apoptotic cellular genes to promote epithelial cell survival. *PLoS Pathog.* 2015;11:e1004979.
58. Kanda T, Miyata M, Kano M, Kondo S, Yoshizaki T, Iizasa H. Clustered microRNAs of the Epstein–Barr virus cooperatively downregulate an epithelial cell-specific metastasis suppressor. *J Virol.* 2015;89:2684–97.
59. Feederle R, Linnstaedt SD, Banner H, Lips H, Bencun M, Cullen BR, et al. A viral microRNA cluster strongly potentiates the transforming properties of a human herpesvirus. *PLoS Pathog.* 2011;7:e1001294.

Publisher's Note Springer Nature remains neutral with regard to jurisdictional claims in published maps and institutional affiliations.

Affiliations

Chan Jin Yoon¹ · Mee Soo Chang²  · Dong Ha Kim¹ · Won Kim³ · Bo Kyung Koo³ · Sung-Cheol Yun⁴ · Sung Han Kim¹ · Yang Soo Kim¹ · Jun Hee Woo¹

¹ Department of Infectious Diseases, Asan Medical Center, Asan Institute for Life Sciences, University of Ulsan College of Medicine, 88 Olympic-ro 43-gil, Songpa-gu, Seoul 05505, Republic of Korea

² Department of Pathology, Seoul National University Boramae Hospital, Seoul National University College of Medicine, 20 Boramae-ro 5-gil, Dongjak-gu, Seoul 07061, Republic of Korea

³ Department of Internal Medicine, Seoul National University Boramae Hospital, Seoul National University College of Medicine, Seoul, Republic of Korea

⁴ Department of Clinical Epidemiology and Biostatistics, Asan Medical Center, University of Ulsan College of Medicine, Seoul, Republic of Korea